Jinst

Published by IOP Publishing for Sissa Medialab

Received: *October 6, 2019*
Revised: *November 15, 2019*
Accepted: *December 13, 2019*
Published: *January 31, 2020*

21st International Workshop on Radiation Imaging Detectors
7–12 July 2019
Crete, Greece

# 3D Diamond Tracking Detectors: numerical analysis for Timing applications with TCAD tools

**A. Morozzi,**[a,1] **S. Sciortino,**[c,d] **L. Anderlini,**[d] **L. Servoli,**[a] **K. Kanxheri,**[a] **S. Lagomarsino**[d] **and D. Passeri**[a,b]

[a] *INFN of Perugia,*
*via Pascoli, 06125 Perugia, Italy*
[b] *Engineering Department — University of Perugia,*
*via G. Duranti 93, 06125 Perugia, Italy*
[c] *Department of Physics — University of Florence,*
*via G. Sansone, 1, 50019 Sesto Fiorentino, Italy*
[d] *INFN of Florence,*
*via G. Sansone, 1, 50019 Sesto Fiorentino, Italy*

*E-mail:* arianna.morozzi@pg.infn.it

Abstract: In view of the HL-LHC upgrade the use of Chemical Vapor Deposited (CVD) diamond has been proposed as an efficient alternative to conventional silicon-based devices. Diamond detectors are more robust to radiation damage, since the high carriers' mobility allows faster signal collection when compared to silicon, while retaining extremely low leakage currents. These properties could be of particular interest in particle detection applications where stringent timing and radiation tolerance requirements need to be fulfilled. A suitable implementation of such a class of detector is that of 3D pixelated CVD diamond with graphitic parallel columns/trenches contact scheme, fabricated through a focused laser beam technology. TCAD simulations can be exploited to assess the effect of different electrode configurations and/or biasing scheme on the electric field profiles, aiming at minimizing the effects of inefficient field regions in terms of charge collection. For timing application purposes, the transport effects along the graphitic columns can be accounted for, aiming at evaluating the performance and limitations of such a class of detectors. The equivalent "load" effect of graphitic columns of different size/resistivity can be taken into account by means of device/circuit-level simulations including measured resistances and capacitances.

Keywords: Detector modelling and simulations II (electric fields, charge transport, multiplication and induction, pulse formation, electron emission, etc); Diamond Detectors; Radiation-hard detectors

[1] Corresponding author.


https://doi.org/10.1088/1748-0221/15/01/C01048

2020 JINST 15 C01048

## Contents



## 1 Introduction

The planned Large Hadron Collider (LHC) upgrade to High Luminosity (HL-LHC) opens the way to a next generation of particle physics experiments and particle detectors, through which extremely high radiation fluence, never experienced before, will be reached [1]. Because of this harsh radiation environment, new technologies for tracking detectors are most likely required.

The adoption of Chemical Vapor Deposited (CVD) diamond devices has been proposed as an efficient alternative to conventional silicon-based detectors in those applications ruled by stringent timing and radiation-tolerance requirements. Indeed, diamond detectors are more robust to radiation damage, and the high carriers' mobility allows faster signal collection when compared to silicon while retaining extremely low leakage currents.

The implementation of 3D-architectures in diamond detectors promises to achieve performances never reached before in radiation-harsh environments [2, 3]. The 3D concept allows for shortening the charge carrier path inside the material, significantly increasing the charge collection efficiency [4]. This feature becomes particularly useful in those detectors with a limited mean free path dominated by trapping mechanisms, such as diamond or silicon sensors after high radiation levels.

In this work, we investigate diamond devices with 3D graphitic columnar electrodes perpendicular to the surface, fabricated using a specialized procedure based on a pulsed laser microfabrication technique in the femtosecond domain [5]. For timing application purposes, the transport effects along graphitic columns have been accounted for, by means of device/circuit-level simulations including measured resistances and capacitances. The concept of distributed resistance along the columnar electrodes has been explored in order to evaluate the performance and limitations of such a class of detectors.

The default material library of the state-of-the-art Synopsys© Advanced TCAD Sentaurus tools does not include diamond, because of the novelty of its use in electronics applications. Nonetheless, a TCAD numerical model describing the electrical properties of polycrystalline CVD (pCVD)



2020 JINST 15 C01048

diamond was recently developed and validated against extensive measurements of planar diamond devices manufactured by different vendors [6–9]. This model has been therefore included within the commercial TCAD environment aiming at predicting the electrical behaviour of more sophisticated devices, such as sensors with 3D architectures fabricated with different diamond qualities. Radiation damage effects can be evaluated as well within the TCAD simulation framework.

This work has been carried out within the framework of the Italian INFN experiment TIMESPOT (TIME and Space real-time Operating Tracker).

## 2 3D diamond devices with graphitic columns

The 3D diamond devices under study are novel detectors fabricated on polycrystalline CVD diamond with resistive graphitic columnar electrodes buried in the bulk. Within the framework of the INFN-TIMESPOT project, the fabricated 3D diamond devices have a cell size of $55 \times 55\ \mu m^2$ and a pitch of 55 μm, in order to be compatible with the dedicated readout electronics. The overall device thickness is 500 μm, and the interdigitated graphitic columns stop at about 50 μm from the opposite surface. The unit cell is composed of a readout electrode at the center and four surrounding electrodes at the corners.

### 2.1 Optimization of the simulated geometry

Within the TCAD environment, the actual 3D diamond device can be approximated, without loss of generality, with a three-dimensional two-cells layout. Indeed a simulation domain composed of two cells is generally the smallest domain which allows accurate simulations in terms of steady-state and active behaviour of the 3D diamond structure, accounting for the interaction of different columnar (ground/bias) electrodes which compete for the carriers collection (figure 1).

For timing application purposes, the suitable modelling of the charge collection mechanisms in terms of time and space is of utmost importance. To this purpose, the mesh elements, where the physical properties of the device are discretized, have to be denser in the more critical regions where the microscopic quantities of interest have a high-density gradient. This requirement translates in a very fine mesh along the particle path and the nearby regions, thus accurately modelling the carriers drift/diffusion dynamics towards the readout electrodes. One main challenge is to find an optimum balancing between simulation accuracy and computational cost, in order to realistically predict the active behaviour of 3D diamond detectors without the need for prohibitive high-performance parallel computing. This goal can be reached by exploiting the symmetry planes of the structure and by considering a quarter of a cell (figure 2). Indeed the electric field profile along the 2D cut of a quarter-cell layout is both qualitatively and quantitatively equal to that of the reference two-cells layout. Figure 3 shows the transverse electric field map with superimposed the set of particle impact points (A-J), which have been selected as representative of the overall detector's response. The stimulus has been modelled as a Minimum Ionizing Particle (MIP) entering the device with normal incidence and uniformly generating 36 pairs/μm along its path. The comparison between the Current-Time (I-t) responses to a MIP read from a two-cells domain and a quarter-cell domain has been selected as the figure of merit, aiming at assessing the suitability of reproducing the 3D diamond detector active behaviour with a simplified layout. The I-t responses resulting from the two-cells and quarter cell domain are illustrated in figure 4, where the coloured lines represent the



2020 JINST 15 C01048

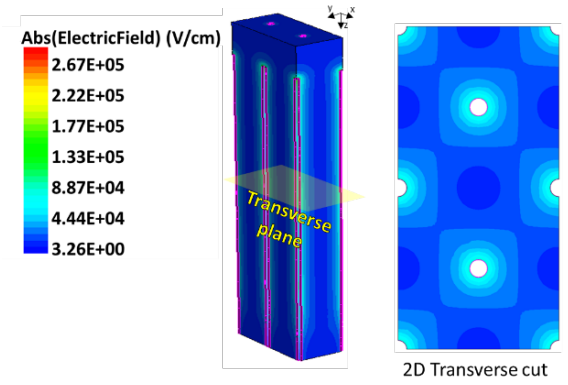


**Figure 1.** Two-cells simulated domain: three-dimensional layout (left), electric field map along the 2D transverse plane at 250 µm from the surface (rigth).

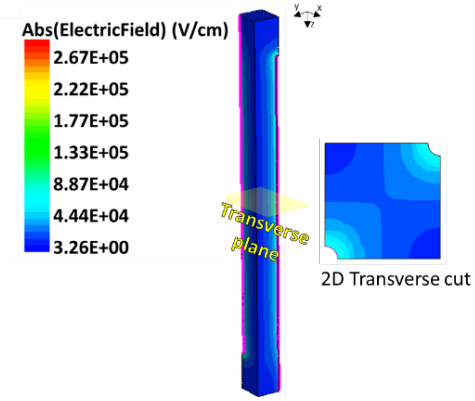


**Figure 2.** Quarter cell simulated domain: three-dimensinal layout (left), electric field map along the 2D transverse plane at 250 µm from the surface (rigth).

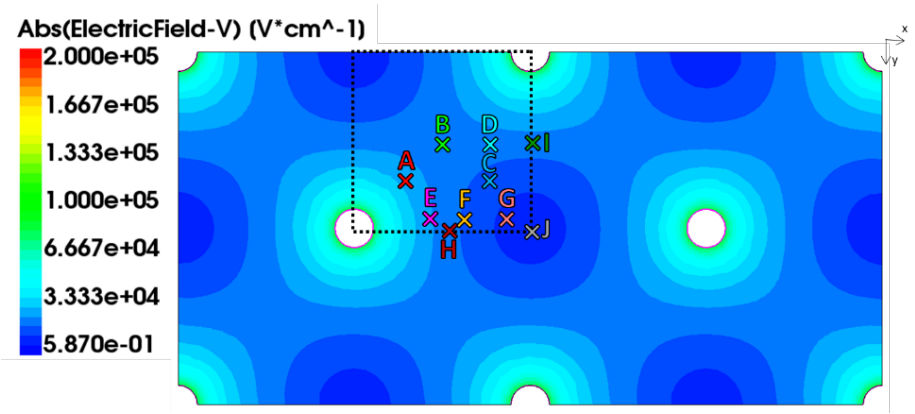


**Figure 3.** Selected impact points (A-J) for the minimum ionizing impinging particle. The considered quarter-cell domain has been enclosed in a black dashed square.

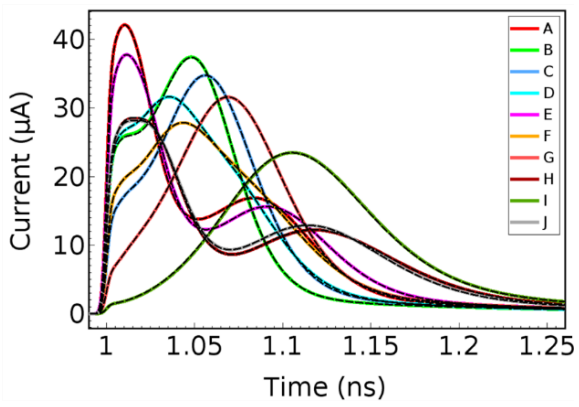


**Figure 4.** Current-time response as a function of an impinging particle at different impact points. Two-cells responses are represented by coloured curves while quarter-cell responses with black dashed curves.

2020 JINST 15 C01048

two-cells structure response, while the black dashed curves represent the quarter-cell response. For corresponding impact points the two sets of curves are entirely overlapping. Taking advantage of this result, a suitable methodology to simulate 3D diamond devices has been devised by exploiting their symmetry planes, thus enhancing the spatial resolution of the simulation results without over-increasing the computational effort.

### 2.2 Small-signal analysis

The implementation of a 3D architecture in diamond devices is pursued with the creation of graphitic buried electrodes by means of laser pulses in the femtoseconds domain [5]. The short pulse length of the laser induces a localized phase transition of the insulating diamond lattice into conductive graphite along columnar paths. The resulting 3D electrodes show fluctuations in the column diameter (tolerance of the production process) which cannot be straightforwardly implemented within the TCAD environment. The graphitic electrodes are therefore modelled as cylinders with an effective diameter value able to reproduce the real device capacitance. Two different geometries have been taken into account: a rectangular cell featuring $114 \times 70\,\mu m^2$as reference and a square cell featuring $55 \times 55\,\mu m^2$ with a pitch compatible to the readout electronics envisaged within the TIMESPOT-INFN project framework. Figure 5 shows the electric field map along the transverse plane at 250 µm from the surface, concerning the rectangular and square cell geometry under investigation and biased at 100 V. At equal biasing voltage, the square geometry shows a smaller extension of low field regions, represented in blue in between the columns. Therefore, the square cell design would foresee a better overall device efficiency in terms of charge collection timing, if compared to the rectangular one.

To reduce the simulation's computational cost, a quarter-cell has been selected as the simulation domain for both the rectangular and square geometries.

Table 1 reports the comparison between measured and simulated capacitance values for the rectangular and square cell geometries. Following the TCAD approach, small-signal (AC) analyses have been carried out at 100 kHz in order to simulate cell capacitance values by considering different effective diameter values. From the experimental point of view, the Capacitance-Voltage (C-V) measurements have been carried out with a HP 4284A PRECISION LCR METER. The structure has been connected by metallizing the signal and bias graphitic tracks on the diamond surface with silver paste and by contacting them with micromanipulators in a mechanical probe station. An open contact measurement has been performed to correct for stray capacitance of the cables. The measurements have been performed at different applied alternate bias voltages at frequencies in the range from 100 Hz to 1 MHz showing substantial frequency independence. The measured capacitance for the rectangular cell geometry $114 \times 70\,\mu m^2$ is 3.0 $pF/mm^2$. This is equivalent to a capacitance of 24 fF per unit cell. This value can be simulated by considering a uniform column diameter of about 5 µm on average for the rectangular cell geometry (table 1). Taking advantage of this result, it is possible to predict the capacitance of cells with different geometries, and it is possible to provide a guideline for the future columns manufacturing process, highlighting the relationship between column diameter reduction and the overall capacitance increase. As an example, at equal column diameter the capacitance of the square cell is about 30% higher than the rectangular cell geometry. This information could be of utmost importance for the readout electronics design.



2020 JINST 15 C01048

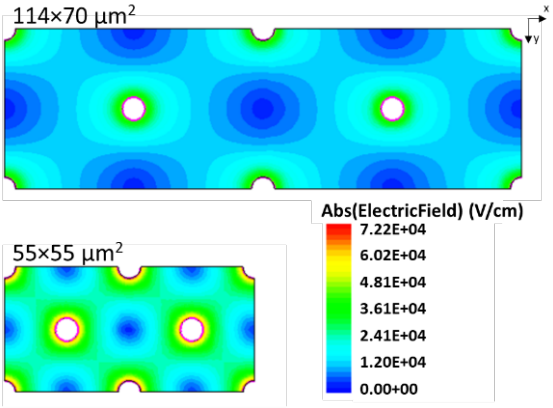


**Figure 5.** Two-cells simulation domain of 3D diamond devices with two different geometries: rectangular $114 \times 70\,\mu m^2$ (top) and square $55 \times 55\,\mu m^2$(bottom) unit cells.

**Table 1.** Measured and simulated capacitance values for the rectangular (reference) and square cell geometry concerning different column diameters ($\phi$).

| Cell size | | | | |
|---|---|---|---|---|
| Rectangular - 114×70 µm | | | Square - 55×55 µm | |
| ϕ (µm) | C (fF/cell) | C (fF/cell) | ϕ (µm) | C (fF/cell) |
| | SIM | MEAS | | SIM |
| 5.0 | 25.2 | 24 | 3.0 | 26.0 |
| 6.0 | 27.0 | | 5.0 | 32.1 |
| 7.5 | 29.5 | | 6.0 | 35.0 |
| 10.0 | 33.5 | | 7.5 | 39.4 |

### 2.3 Modelling of the transport along the columns

When a particle crosses the active sensor volume, it releases enough energy to generate free electron-hole pairs along its path, which are then collected by the read-out graphitic electrodes under the effect of the electric field. Hence, a meaningful physical description of the detector's electric field is mandatory to simulate and predict the mechanism of charge collection, realistically.. Moreover, the charge transport along the graphitic electrode toward the read-out circuitry has to be taken into account and modelled, especially for timing applications purposes.

#### 2.3.1 Sensitivity to the column's conductivity

The numerical model for the material graphite is not included within the default material's library of the TCAD environment. In this work, the 3D columnar graphite electrodes have been therefore described with an ad-hoc customized parametric file modelling the column conductivity. Moreover, the TCAD simulation tools model the contacts as equipotential lines/surfaces in 2/3-dimensions where to apply specific thermal/electrical boundary conditions. In this work, the equipotential readout contacts are located on opposite diamond surfaces for biased/grounded columns (magenta lines in figure 6 and figure 7) and the non-ideality related to the transport along the columns are entirely ascribed to the conductivity properties of the material composing the columns. The electric field (V/cm) and the total current density distribution ($A/cm^2$) have been selected as representative physical quantities to describe and to differentiate between the metal and insulating behaviour of the material composing the columns. A huge range of resistivity values between $10^{-05}\,\Omega m$ and $10^{+22}\,\Omega m$ have been explored, spanning from near-metallic (e.g. graphite) to insulating material (e.g. pure diamond). The simulation domain of figure 6 and figure 7 is a longitudinal cut of the simulated 3D diamond detector along the diagonal that connects two columns differently polarized (0 and 100 V). Figure 6 shows the electric field distribution, which represents a key feature to analyse and predict the charge collection dynamics depending on the particle impact point. Indeed in figure 6(a) and 6(b) the ionized charge, under the effects of a high electric field, shortly drift



2020 JINST 15 C01048

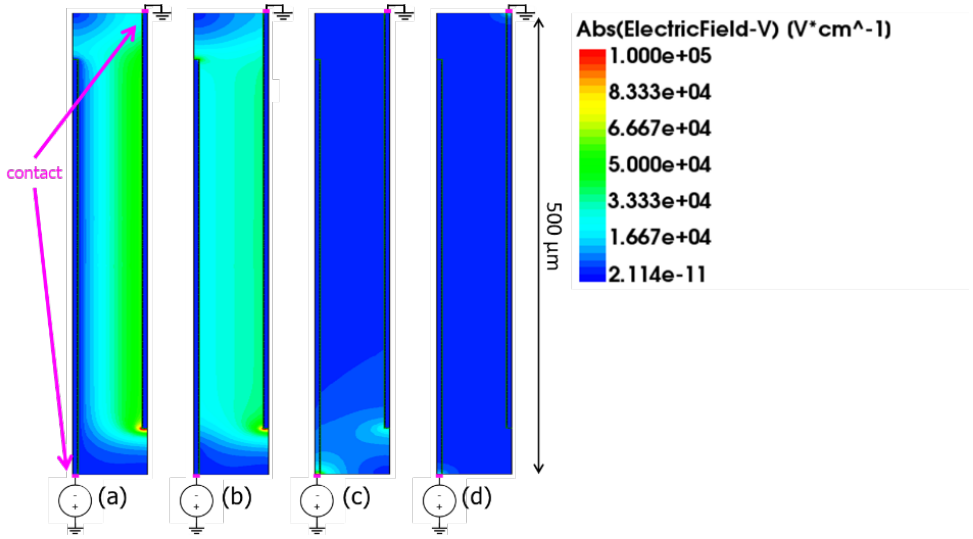


**Figure 6.** Electric field as a function of the column resistivity: $1.1\times10^{-05}$ (a), $1.4\times10^{-02}$ (b), $1.0\times10^{-02}$ (c), $9.6\times10^{+23}$ (d) Ωm.

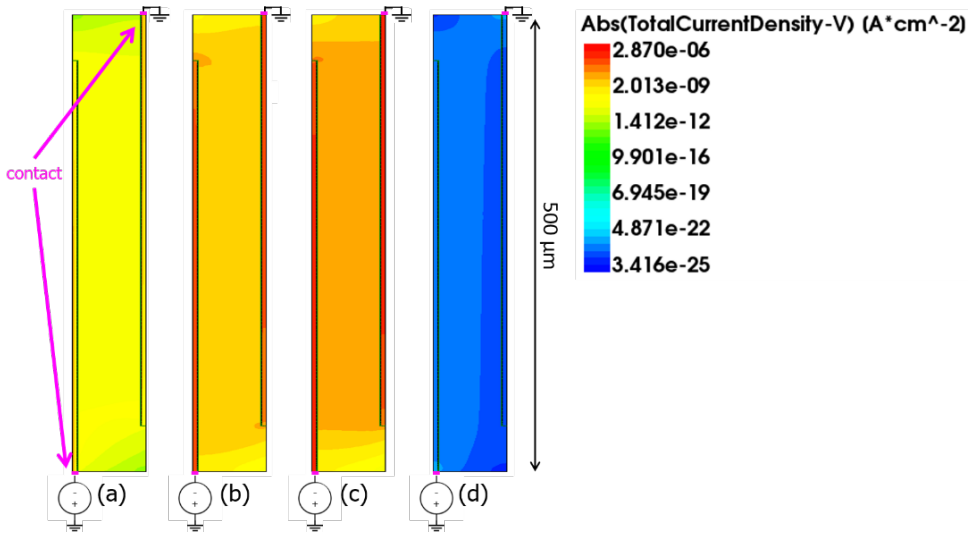


**Figure 7.** Total current density as a function of the column resistivity: $1.1\times10^{-05}$ (a), $1.4\times10^{-02}$ (b), $1.0\times10^{-02}$ (c), $9.6\times10^{+23}$ (d) Ωm.

towards the columns. Differently, the low electric field region that affects the whole device in figure 6(c) and 6(d), introduces a prolongation of the collection time. The goal is to find a suitable column conductivity value for simulation purposes, and this can be pursued by means of an extensive comparison between simulation and measurements. This enables a realistic modelling of the steady-state and active behaviour of 3D diamond detectors.

### 2.3.2 Implementation of the distributed resistance

The current-time (I-t) signal timing properties are affected by the 3D column conductivity properties. The signal rise time can be adjusted by the value of distributed resistance associated with the contact, expressed in $\Omega\times cm^2$. This concept paves the way towards tunable TCAD numerical model of 3D



2020 JINST 15 C01048

diamond detectors to reproduce experimental data in terms of signal duration and rise-time as a response to a particle hit.

A Minimum Ionizing Particle (MIP) passes through the diamond device producing roughly uniform electron-hole pairs along its path. In order to study the impact of the charge transport along the columns on the active behaviour of diamond devices, and in particular on the charge collection timing, a concentrated stimulus has been used as input signal at different distances from the readout electrode (figure 8). In this way it is possible to study how the different signal contributions are processed depending on the distance between the produced ionized charges and the collection electrodes.

The stimulus releases 2.8 fC, which represents the equivalent charge generated by a MIP in 500 μm of a diamond substrate, concentrated in a spot size of $4 \times 1$ μm$^2$. Figure 9 reports the readout contact I-t responses concerning the spots A and B and in two operating cases: with (dashed lines) and without (solid lines) the activation of the distributed resistance at contacts. The activation of the distributed resistance acts as a resistive load applied at contacts and it has an effect on the transient current signal rise-time without significantly affecting its shape.

The total current density is the sum of three components: the electron current density, the hole current density and the displacement current density. The transient current signal is generated from the displacement of electric charges moving inside the space charge region, even though there have not been yet collected by the electrodes [10]. In all the curves reported in figure 9 two peaks are clearly visible and in particular, the first one is related to the perturbation induced by the generated charge on the electrode, as just described, and the second peak, instead, is the result of the electron current density due to the arrival of carriers (electrons) at the readout electrode. Due to the applied polarization, the readout electrode collects electrons. The two concentrated spots A and B are 30 μm and 20 μm away from the opposite surfaces, respectively. As a consequence, the first peak arises earlier (blue curves) since the B spot is closer to the biasing electrode and therefore is more affected by the instantaneous charge induction. On the other hand, the second peak is faster for the spot A since it is closer to the (electrons) readout electrode. As expected, the closer the generated charge to the readout electrode (point A), the faster the collection mechanism.

Eventually, the modelling of the contacts with a distributed resistance allows the simulation of a more realistic signal rise-time.

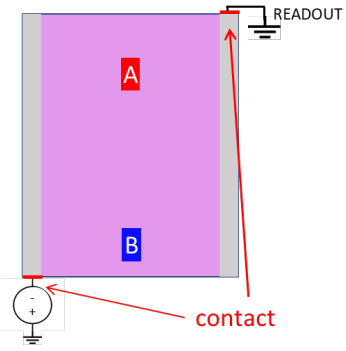


**Figure 8.** Two particle impact points A and B at different distances from the readout electrode.

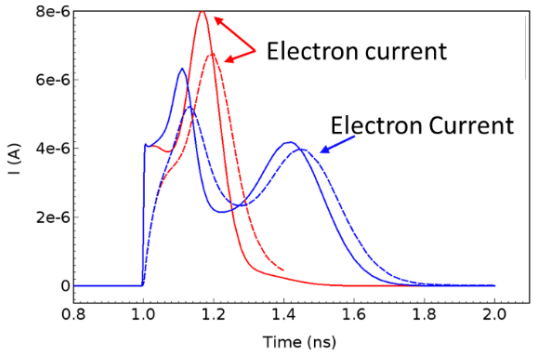


**Figure 9.** I-t response to spot A (red) and B (blue) with (dashed lines) and without (solid lines) the activation of the distributed resistance of $0.05\,\Omega \times \mathrm{cm}^2$ at contacts.

2020 JINST 15 C01048

## 3 Conclusion

In this work, a numerical methodology to simulate the steady-state and active responses of 3D diamond detectors has been proposed. An already developed numerical TCAD model of polycrystalline diamond for the simulations of general-purpose diamond-based devices has been applied to the investigation of more sophisticated devices characterized by 3D-architectures.

Without loss of generality, the simulation domain has been simplified to a quarter of cell, exploiting the symmetry planes of the device. This technique becomes very beneficial for timing application purposes, where high spatial resolution and therefore very dense mesh are mandatory to perform accurate simulations. A suitable balance between spatial resolution and simulation domain can be therefore obtained, to reduce the computational load upon the system, while maintaining the required level of accuracy of the simulation.

The effects related to the charge transport along the buried graphitic electrodes can be taken into account by properly considering the conductivity of 3D graphitic columnar electrodes together with the distributed resistivity associated with contacts. This represents a suitable methodology to obtain realistic and physically meaningful simulation results.


## Acknowledgments

This work has been carried out within the framework of the Italian INFN experiment TIME and Space real-time Operating Tracker (TIMESPOT).


## References


[1] CERN, *HL-LHC: High luminosity large hadron collider*, https://hilumilhc.web.cern.ch (2015).

[2] H. Kagan, *Diamond detector technology, status and perspectives*, *Nucl. Instrum. Meth.* **A 924** (2019) 297.

[3] F. Bachmair et al., *A 3D diamond detector for particle tracking*, *Nucl. Instrum. Meth.* **A 786** (2015) 97 [*Erratum ibid.* **A 797** (2015) 331].

[4] S. Lagomarsino, M. Bellini, C. Corsi, V. Cindro, K. Kanxheri, A. Morozzi et al., *Radiation hardness of three-dimensional polycrystalline diamond detectors*, *Appl. Phys. Lett.* **106** (2015) 193509.

[5] S. Lagomarsino, M. Bellini, M. Brianzi, R. Carzino, V. Cindro, C. Corsi et al., *Polycrystalline diamond detectors with three-dimensional electrodes*, *Nucl. Instrum. Meth.* **A 796** (2015) 42.

[6] A. Morozzi, D. Passeri, K. Kanxheri, L. Servoli, S. Lagomarsino and S. Sciortino, *Polycrystalline CVD diamond device level modeling for particle detection applications*, 2016 *JINST* **11** C12043.

[7] A. Morozzi, D. Passeri, K. Kanxheri, L. Servoli, S. Sciortino and S. Lagomarsino, *Numerical modelling of polycrystalline diamond device for advanced sensor design*, *Mater. Today Proc.* **3** (2016) S153.

[8] A. Morozzi, D. Passeri, S. Vecchi, L. Servoli and S. Sciortino, *Combined TCAD and geant4 simulations of diamond detectors for timing applications*, *Nucl. Instrum. Meth.* **A 936** (2019) 436.

[9] A. Morozzi and D. Passeri, *A TCAD modeling approach for diamond particle detectors: Simulation and test*, in proceedings of *13th Conference on Ph.D. Research in Microelectronics and Electronics (PRIME)*, Giardini Naxos, Italy, 12–15 June 2017, pp. 73–76.

[10] W. Shockley, *Currents to conductors induced by a moving point charge*, *J. Appl. Phys.* **9** (1938) 635.




2020 JINST 15 C01048